Hydration state and activity of aqueous silica in H_2O-CO_2 fluids at high pressure and temperature

ROBERT C. NEWTON AND CRAIG E. MANNING*

Department of Earth and Space Sciences, University of California at Los Angeles, Los Angeles, California 90095, U.S.A.

ABSTRACT

Quartz solubility in H_2O-CO_2 fluids was measured at 800 °C and 10 kbar. Mixed fluids were generated from hydrous oxalic acid, silver oxalate, silver carbonate, and liquid H_2O; solubility was determined by weight changes of the quartz crystals. Stringent blank tests and weighing procedures were used to establish the CO_2 and H_2O contents of experimental fluids. Using experimentally constrained models of H_2O activity and mixing of silica monomers and dimers, a logarithmic plot of monomer activity vs. H_2O activity yields a linear data array of constant slope n insignificantly different from 4 ($n = 4.024$, $R^2 = 0.997$), where n is the total monomer hydration number. Moreover, all high-quality quartz solubility data in H_2O-CO_2 fluids at lower temperature and pressure fall on the same line when SiO_2 and H_2O activities are calculated with this formulation. The same analysis for the dimer yields slope n of 7 ($n = 7.049$, $R^2 = 0.996$). Our results show that neutral silica monomers and dimers have fixed stoichiometry of $Si(OH)_4 \cdot 2H_2O$ and $Si_2O(OH)_6 \cdot 4H_2O$ (i.e., two solvating H_2O molecules per Si) in H_2O-CO_2 fluids for a large range of crustal metasomatic processes. This provides a simple basis for modeling H_2O-CO_2-SiO_2 fluids over a range of pressure, temperature, CO_2, and SiO_2 activity.

Keywords: Quartz solubility, crustal fluids, experimental petrology, thermodynamics

INTRODUCTION

H_2O and CO_2 are major molecular components of crustal fluids, and silica is among the most abundant solutes. The determination of quartz solubility in H_2O-CO_2 fluids at high temperatures and pressures is therefore essential to the study of fluid-mediated mass transfer. Experimental studies (Shettel 1974; Novgorodov 1975; Walther and Orville 1983; Newton and Manning 2000; Shmulovich et al. 2001, 2006) observed that at 400–800 °C and 1–10 kbar, quartz solubility declines greatly as CO_2 increases in the fluid phase. This demonstrates that the compositions of H_2O-CO_2 fluids during igneous and metamorphic processes will influence associated material transport in the crust.

Quartz solubility is controlled by its interaction with fluid components. Because solute silica does not form complexes with CO_2, observed variations with pressure (P), temperature (T), and CO_2 mole fraction (X_{CO_2}) can be attributed mainly to changes in H_2O activity. Walther and Orville (1983) showed that solvation of dissolved silica by H_2O molecules could be assessed quantitatively by writing the quartz dissolution reaction as:

$$SiO_2 + nH_2O = Si(OH)_4 \cdot (n-2)H_2O \qquad (1)$$
$$\text{quartz} \qquad\qquad \text{solute complex}$$
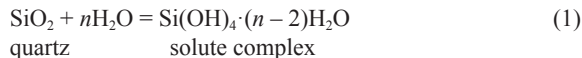
which accounts for two moles H_2O as hydroxyls and $n - 2$ moles of molecular H_2O of solvation per mole of solute silicon. The number of H_2O of solvation can be determined from quartz solubility data by the relation $n = d\log a_{Si(OH)_4 \cdot (n-2)H_2O} / d\log a_{H_2O}$ at constant P and T. Previous work had been inconclusive about the silica hydration state, but Walther and Orville (1983) showed that, assuming all silica dissolved as monomeric $Si(OH)_4$ in their

H_2O-CO_2 experiments, plots of log silica molality (m_{SiO_2}) vs. log H_2O mole fraction (X_{H_2O}) give $n \approx 4$ (i.e., two molecular H_2O of solvation) for many conditions, though uncertainties in n were at least ±1. Subsequent studies suggested explicitly or implicitly that n is instead 3.5 or 2 (Shmulovich et al. 2006; Akinfiev and Diamond 2009), or that it decreases with increasing X_{CO_2} at constant P and T (Newton and Manning 2000; Shmulovich et al. 2001). Similar uncertainty exists for H_2O-Ar solutions (Crerar and Anderson, 1971; Walther and Orville, 1983). Resolution of the debate has been limited by widely varying accuracy and precision of solubility data, by a lack of H_2O-CO_2 mixing models that could provide sufficiently accurate a_{H_2O}, and by the previously unrecognized polymerization of aqueous silica at high P and T (e.g., Zotov and Keppler 2002; Newton and Manning 2002). However, recent results encourage renewed focus on the hydration state of aqueous silica in CO_2-H_2O fluids. Aranovich and Newton (1999) derived thermodynamic mixing properties in CO_2-H_2O fluids to 15 kbar and 1000 °C, and over a large composition range. Newton and Manning (2002, 2003) also developed an experimentally constrained activity model for aqueous silica from 1–14 kbar at 600–900 °C, which accounts for polymerization. Thus, the activities of both H_2O and SiO_2 can now be independently represented in H_2O-CO_2 mixtures.

The present study gives new, high-precision measurements of SiO_2 concentrations at quartz saturation at 800 °C, 10 kbar, and CO_2 concentrations up to 93 mol%. The study is made possible by new methods of characterization of CO_2-H_2O fluids and by precise measurement of quartz solubility using an ultramicrobalance and the rapid-quench capabilities of the piston-cylinder apparatus. Our results demonstrate that hydration of silica species is invariant over a wide P-T range where H_2O and CO_2 are miscible, leading to a simple model for quartz solubility in crustal H_2O-CO_2 fluids.

* E-mail: manning@ess.ucla.edu

EXPERIMENTAL METHODS

Quartz solubility measurements were carried out by the rapid-quench, hydrothermal piston-cylinder techniques of Manning (1994) and Newton and Manning (2000), using the same quartz source and methods. Starting materials were contained in Pt capsules of 3.5 mm OD and 0.20 mm wall thickness. Fluid charges were prepared from three CO_2 sources, with or without additional H_2O: hydrous oxalic acid, $H_2C_2O_4\cdot2H_2O$ (HOX), silver oxalate, $AgCO_2$, (AgOX), and silver carbonate (Ag_2CO_3). AgOX was found to be slightly hydrous (Ferry et al. 2002), which led to minor corrections to fluid composition (Table 1 and Supplementary data[1]). Volatile yield tests on several quenched capsules were performed after dissolution experiments by a freezing/timed-weight-loss technique. The results agreed with expected CO_2 and H_2O yields (Table 1). When combined with propagated weighing errors, the CO_2 and H_2O contents of the experimental fluid are accurate to better than 0.1 mol%. Silver-CO_2 species are assumed to be negligible. Solute silica concentrations were determined to high precision from crystal weight losses ($1\sigma = 0.2$ μg).

RESULTS

Figure 1a shows SiO_2 molality (m_{SiO_2}) vs. X_{H_2O} for all experiments of the present study using different combinations of CO_2 and H_2O sources (Table 1). The SiO_2 concentration decreases strongly and systematically with decreasing H_2O.

Equilibrium quartz solubility can be assumed in the runs based on: (1) only ~2 h are needed for equilibrium between quartz and H_2O at 700 °C and 10 kbar (Newton and Manning 2000); (2) m_{SiO_2} at $X_{CO_2}= 0.5$ from two different starting fluid sources are nearly identical; and (3) results of experiments of duration varying by a factor of five plot on the same trend. One Ag_2CO_3 run (QZ-41, Table 1) has an anomalously large volatile yield discrepancy and plots off the trend defined by the other data (Fig. 1a); however, it is retained in the data set. Experiment QZ-44 ($X_{CO_2} = 0.07$) had weight loss below detection limits (Table 1, Fig. 1a); this datum is omitted from further consideration.

---

[1] Deposit item AM-09-042, Supplementary data, tables, and figure. Deposit items are available two ways: For a paper copy contact the Business Office of the Mineralogical Society of America (see inside front cover of recent issue) for price information. For an electronic copy visit the MSA web site at http://www.minsocam.org, go to the American Mineralogist Contents, find the table of contents for the specific volume/issue wanted, and then click on the deposit link there.

DISCUSSION

Figure 1b shows that the new data are substantially more precise than our previous results (Newton and Manning 2000). The average deviation from a quartic regression is 6%, whereas the previous data display much larger deviations.

The importance of improved precision is seen by comparing the present data to predictions of Akinfiev and Diamond (2009) and Shmulovich et al. (2006), who used:

$$\log m_{SiO_2} = \log m'_{SiO_2} + n\log X_{H_2O} \qquad (2)$$

where m'_{SiO_2} is the molality in H_2O at any P and T, and n is the total hydration number (Eq. 1). Shmulovich et al. (2006) adopted $n = 3.5$ at 800 °C and 5 kbar, and Akinfiev and Diamond (2009) chose $n \sim 2$. These give reasonable forms to the m_{SiO_2}-X_{H_2O} function (Fig. 1a) and are broadly consistent with earlier lower precision results, but both models show considerable, systematic discrepancies from the present experimental data (Fig. 1b).

With the new data, a more robust derivation of n can be attempted. Obtaining n from the experiments requires calculation of activities of silica and H_2O. Silica activity may be evaluated using the model of Newton and Manning (2002, 2003), in which H_2O of solvation is implicit. At crustal P and T, homogeneous equilibrium in an H_2O-SiO_2 fluid can be written

$$2Si(OH)_4 = Si_2O(OH)_6 + H_2O \qquad (3)$$
$$\text{monomer} \qquad \text{dimer}$$
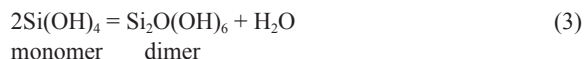
(Zotov and Keppler 2002; Newton and Manning 2002, 2003). By equating activities of the monomer (m) and dimer (d) to their mole fractions, the equilibrium constant for Equation 3 (K_{md}) is

$$K_{md} = \frac{X_d a_{H_2O}}{X_m^2} \qquad (4)$$

For results where H_2O is the only solvent component, $a_{H_2O} \approx 1$. With this assumption, least-squares regression of K_{md} values of Newton and Manning (2002) gives:

$$\log K_{md} = 1.480 + 0.0012T + (0.000119T - 0.165)P \qquad (5)$$

where T is in K and P is in kbar. This formula leads to $K_{md} = 229$
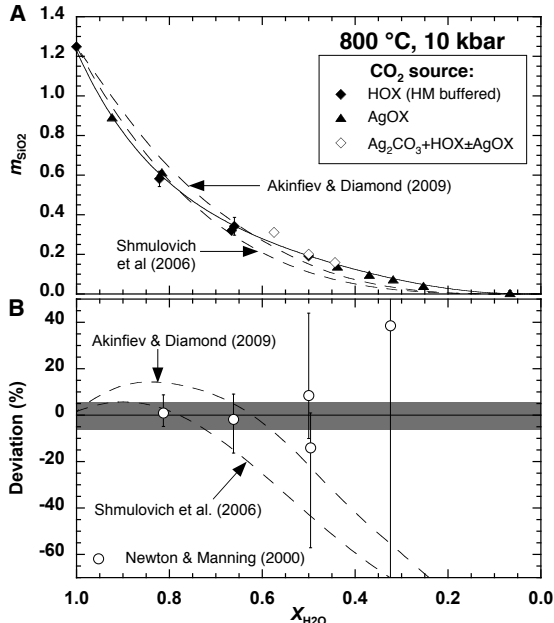
TABLE 1. Experimental results

Expt. no.	Run time (h)	Ag_2CO_3 in	HOX in*	AgOX in	H_2O in	Total H_2O in†	Total CO_2 in	X_{H_2O} in	a_{H_2O}	Quartz weight loss	m_{SiO_2}	$\log a_{SiO_2}$	H_2O out‡	CO_2 out‡	Total fluid out‡	Δ§
QZ-25	17			19.106	25.95	26.081	5.288	0.9234	0.9340	1.3993	0.8921(03)	−2.343(21)				
C-5	46		1.85		1.906	2.435	1.292	0.8216	0.8664	0.085	0.581(19)	−2.498(22)	2.382	1.335	3.717	−0.009
QZ-28	17			44.893	22.241	22.604	12.425	0.8163	0.8632	0.8350	0.6148(05)	−2.485(21)	22.173	12.93	35.103	0.056
QZ-20	12		4.158		1.185	2.373	2.903	0.6663	0.7749	0.0457	0.3202(20)	−2.736(21)			5.284	0.007
C-4	45		3.774		1.014	2.093	2.635	0.6599	0.7710	0.043	0.342(22)	−2.721(25)	2.108	2.631	4.739	0.011
QZ-41	18	42.529	19.408		2.932	11.257	20.338	0.5748	0.7156	0.2102	0.3108(04)	−2.799(21)			31.912	0.317
QZ-36	5	24.967	11.725			4.987	12.171	0.5002	0.6601	0.0602	0.2008(09)	−2.980(21)			17.157	−0.001
QZ-19	19		6.429			1.837	4.489	0.5000	0.6599	0.0211	0.1914(26)	−2.995(21)			6.376	0.050
QZ-39	5.5	40.436	18.467	19.546		8.078	24.757	0.4435	0.6123	0.0770	0.1586(06)	−3.100(21)			32.806	−0.036
QZ-29	24			55.781	4.472	4.923	15.438	0.4379(1)	0.6072(2)	0.0410	0.1387(12)	−3.148(21)	4.451	15.682	20.133	−0.250
QZ-30	16			53.143	3.1	3.530	14.708	0.3696(1)	0.5414(2)	0.0207	0.0975(15)	−3.332(21)				
QZ-43	7.5			61.339	2.744	3.240	16.976	0.3180(1)	0.4855(2)	0.0145	0.0745(16)	−3.487(21)	3.214	16.953	20.167	−0.074
QZ-31	16			56.024	1.694	2.147	15.505	0.2528(2)	0.4066(2)	0.0053	0.0413(22)	−3.797(24)	2.051	15.584	17.635	−0.040
QZ-44	18			106.284		0.859	29.415	0.0666(2)	0.1238(4)	0.0003	0.0058(55)‖				30.108	−0.166

Note: All weights in milligrams. Weights to 3 decimal places determined on a Mettler M3 ($1\sigma = 2$ μg); weights to 4 decimal places determined on a Mettler UMX2 ($1\sigma = 0.2$ μg); parenthetical entries are 1σ in last digit(s) as calculated by propagation of weighing errors (only shown when ≥1 in last digit).
* HOX runs were f_{O_2}-buffered at hematite-magnetite equilibrium (see Supplementary data[1]).
† Calculated fluid compositions assume that all excess H_2 from HOX is absorbed by the HM buffer or reacted to H_2O in the runs with Ag_2CO_3, and include 2.79% of expected CO_2 yield from AgOX as H_2O (Table S1[1]).
‡ Volatile contents determined by drying-loss analysis of the fluids from quenched capsules.
§ Δ = (H_2O in − H_2O out) + (CO_2 in − CO_2 out), in milligrams. Agreement between post-run drying-loss analysis with the fluid compositions calculated from loaded starting materials demonstrates accuracy of reported fluid compositions (see Supplementary data[1]).
‖ Quartz solubility in Experiment QZ-44 is below 3σ detection limit of 0.6 μg weight loss.

FIGURE 1. (**a**) Variation in molality of SiO_2 with X_{H_2O} at 800 °C and 10 kbar. Data from Table 1 (2σ errors). The data are reproduced by a simple three-parameter fit equation $X_{SiO_2}^{1/4} = 0.5930 X_{H_2O} - 0.5303 X_{H_2O}^2 + 0.3211 X_{H_2O}^3$ ($R^2 = 0.997$). Shown also are solubilities predicted by Shmulovich et al. (2006) and Akinfiev and Diamond (2009). HM = Hematite-magnetite; see Supplementary data[1] for discussion of fluid compositions. (**b**) Deviation of predicted or measured solubility from best fit to experiments (solid line, from **a**). Shaded area is 6% deviation from fit equation; open circles from Newton and Manning (2000; 1σ errors).

at 800 °C and 10 kbar. Values of a_{SiO_2} for the present experiments in H_2O-CO_2 mixtures, where $a_{H_2O} < 1$, can be computed using this value of K_{md} by taking the standard state of total dissolved SiO_2 to be unit activity of the pure hypothetical solution of monomers, such that:

$$a_{SiO_2} = \gamma_{SiO_2} X_{SiO_2} = X_m = a_m \qquad (6)$$

where γ_{SiO_2} is the activity coefficient of aqueous SiO_2. As shown by Newton and Manning (2006), Equations 4 and 6 lead to:

$$a_{SiO_2} = \frac{\left(1 + 8 X_{SiO_2} K_{md} / a_{H_2O}\right)^{1/2} - 1}{4 K_{md} / a_{H_2O}} \qquad (7)$$

Figure 2a shows log a_{SiO_2} calculated for the present experimental results, with log a_{H_2O} from Aranovich and Newton (1999). A linear fit to the rest of the data yields $n = 4.024$ ($R^2 = 0.997$). There is coherence of the data from all three kinds of starting material. The value of K_{md} is somewhat uncertain, but extreme values of 100 and 300 also yield linear fits, high R, and n of 4.2 and 3.8, respectively. Subtraction of H_2O bound in solute silica from bulk H_2O has negligible effect on the calculations; H_2O activities were therefore calculated from total H_2O contents.

The data imply that the total hydration number n is effectively an integer (Walther and Orville 1983), which presumably corresponds to a discrete solvation complex of fixed stoichiometry. On the basis of Figure 2a, we may take n at 800 °C, 10 kbar to be four—two H_2O molecules consumed to form hydroxyls of silicic acid, and two molecular H_2O of solvation—correspond-

ing to a monomer formula of $Si(OH)_4 \cdot 2H_2O$. This conclusion, though never previously documented as thoroughly, agrees with the deductions of Walther and Orville (1983). An identical analysis shows that n for the dimer of 7.049 ($R^2 = 0.996$; Fig. 2b) is obtained if the stoichiometry of Equation 3 is as written; alternative versions involving more or fewer H_2O of dehydration yield substantially poorer fits. The dimer has 6 OH⁻, so $n = 7$ gives $Si_2O(OH)_6 \cdot 4H_2O$; i.e., 4 molecular H_2O of solvation, or 2 per Si as in the monomer.
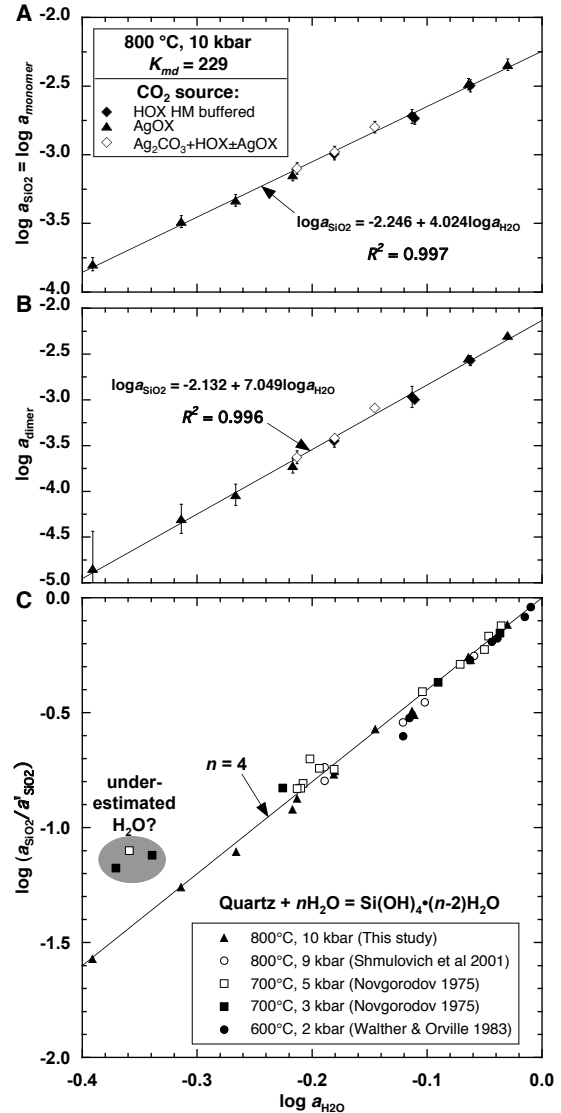

FIGURE 2. (**a**) Logarithmic plot of SiO_2 activity (a_{SiO_2}) vs. H_2O activity (a_{H_2O}) in the experiments of this study. Symbols denote CO_2 sources (2σ errors). The slope of 4 argues for a monomer formula of $Si(OH)_4 \cdot 2H_2O$. (**b**) Logarithmic plot of dimer activity vs. a_{H_2O}. Symbols as in **a** (2σ errors). The slope of 7 indicates a dimer formula of $Si_2O(OH)_6 \cdot 4H_2O$. (**c**) Logarithmic plot of the ratio of a_{SiO_2} in mixed fluids to that in pure H_2O (a'_{SiO_2}) vs. a_{H_2O} in published high-precision, quartz-saturated experimental data. A linear fit with an assumed intercept of zero gives n very close to 4, indicating monomer stoichiometry of $Si(OH)_4 \cdot 2H_2O$ over a broad P-T range. The data of Novgorodov (1975) at the highest CO_2 (circled) depart from the trend due to probable inaccuracy in determination of fluid composition (see text).
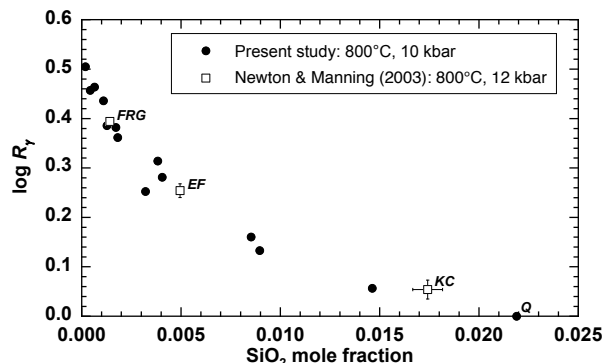
Figure 3. Logarithm of the ratio of the activity coefficient of SiO_2 at quartz saturation in mixed fluids to that in pure H_2O (R_γ) vs. X_{SiO_2} at 800 °C and 10 kbar. Also shown are R_γ values at 800 °C, 12 kbar (Newton and Manning 2003) for four buffering assemblages in pure H_2O: Q = quartz; KC = corundum-kyanite; EF = enstatite-forsterite; and FRG = forsterite-rutile-geikielite (2σ errors).

The constancy of two H_2O of solvation per aqueous Si over crustal conditions may be explored by comparison with the data of Novgorodov (1975), Walther and Orville (1983), and Shmulovich et al. (2001) at lower P and T. All other determinations lack precision sufficient to yield meaningful constraints. Figure 2c shows log a_{SiO_2} vs. log a_{H_2O} over a range of P and T, with a_{SiO_2} normalized to that in H_2O (a'_{SiO_2}) to allow comparison (Table S2[1]). All data together indicate that n is near 4, with the exception of Novgorodov's (1975) results at high X_{CO_2} (Fig. 2c). Novgorodov allowed CO_2 to escape from his capsules at room T (rather than while H_2O was frozen), which could cause some H_2O to be lost in the CO_2 efflux and give spuriously high X_{CO_2}. That these data are suspect is supported by our measured solubility of <0.003 wt% at $X_{CO_2} = 0.93$ (QZ-44, Table 1), which in spite of higher P and T is much lower than Novgorodov's value of 0.018 wt% at 700 °C, 5 kbar, and $X_{CO_2} = 0.96$. Thus, neglecting circled data in Figure 2c, the total hydration number of monomeric silica is apparently 4 (and of the dimer, 7), independent of T, P, or a_{H_2O}, to at least 800 °C, 10 kbar, and X_{CO_2} at least 0.75.

The conclusion that the monomer and dimer possess constant solvation stoichiometry has important implications for systems with reduced a_{SiO_2}. Equilibrium dictates that, for reaction 1 in CO_2-H_2O fluids ($a_{H_2O} \neq 1$):

$$0 = \Delta G° + RT\ln\gamma_{SiO_2} + RT\ln X_{SiO_2} - 4RT\ln a_{H_2O} \quad (8)$$

for $n = 4$, where $\Delta G°$ is the standard state Gibbs energy change. In contrast, in pure H_2O ($a_{H_2O} \approx 1$):

$$0 = \Delta G° + RT\ln\gamma'_{SiO_2} + RT\ln X'_{SiO_2} \quad (9)$$

where a prime again refers to a quantity in the CO_2-absent system. Equations 8 and 9 lead to

$$\log R_\gamma = \log\left(\frac{\gamma_{SiO_2}}{\gamma'_{SiO_2}}\right) = 4\log a_{H_2O} - \log\left(\frac{X_{SiO_2}}{X'_{SiO_2}}\right) \quad (10)$$

where R_γ is the SiO_2 activity coefficient in any solution relative to that at quartz saturation in pure H_2O and the same P and T, whether the change in a_{SiO_2} is caused by decrease of a_{H_2O} at quartz saturation (this study) or by buffering of a_{SiO_2} at values below quartz saturation in pure H_2O (Newton and Manning 2002, 2003). Figure 3 demonstrates that R_γ values derived from this study agree with those found by Newton and Manning (2003)

for several buffering assemblages in pure H_2O at 800 °C and 12 kbar. The intercept at $X_{CO_2} = 1$ is the logarithm of the reciprocal of the activity coefficient of SiO_2 in pure H_2O.

Figure 3 shows that reduction of SiO_2 activity by addition of CO_2 to quartz-saturated H_2O or by buffering SiO_2-H_2O fluid below quartz saturation has the same functional form. Thus, adopting $n = 4$ for the monomer and $n = 7$ for the dimer allows quantitative calculation of species activities and H_2O solvation for metasomatic processes involving quartz-saturated and/or quartz-undersaturated H_2O-CO_2 fluids over a wide range of crustal P-T. Moreover, for the experimentalist, measured quartz solubility in CO_2-H_2O fluids at high P and T provides a sliding-scale monitor of SiO_2 activity over a considerable range of P and T. The free energies of formation of some silicates may be measured by their solubilities in CO_2-H_2O fluids at high P and T, at least for those minerals for which the other components are much less soluble than SiO_2 and which do not complex with CO_2 (e.g., Al-silicates or zircon). Quartz solubility in CO_2-H_2O fluids provides a baseline for the solution behavior of silica when H_2O activity is the controlling factor; departure from this baseline highlights possible silica complexing with other solute components.

References Cited

Akinfiev, N.N. and Diamond, L.W. (2009) A simple predictive model of quartz solubility in water-salt-CO_2 systems at temperatures up to 1000 °C and pressures up to 1000 MPa. Geochimica et Cosmochimica Acta, 73, 1597–1608.
Aranovich, L.Y. and Newton, R.C. (1999) Experimental determination of CO_2-H_2O activity-composition relations at 600–1000 °C and 6–14 kbar by reversed decarbonation and dehydration reactions. American Mineralogist, 84, 1319–1332.
Crerar, D.A. and Anderson, G.M. (1971) Solubility and solvation reactions of quartz in dilute hydrothermal solutions. Chemical Geology, 8, 107–122.
Ferry, J.M., Newton, R.C., and Manning, C.E. (2002) Experimental determination of the equilibria: rutile + magnesite = geikielite + CO_2 and zircon + 2magnesite = baddeleyite + forsterite + 2CO_2. American Mineralogist, 87, 1342–1350.
Manning, C.E. (1994) The solubility of quartz in H_2O in the lower crust and upper mantle. Geochimica et Cosmochimica Acta, 58, 4831–4839.
Newton, R.C. and Manning, C.E. (2000) Quartz solubility in H_2O-NaCl and H_2O-CO_2 solutions at deep crust-upper mantle pressures and temperatures: 2–15 kbar and 500–900 °C. Geochimica et Cosmochimica Acta, 64, 2993–3005.
——— (2002) Solubility of enstatite + forsterite in H_2O at deep crust/upper mantle conditions: 4 to 15 kbar and 700 to 900 °C. Geochimica et Cosmochimica Acta, 66, 4165–4176.
——— (2003) Activity coefficient and polymerization of aqueous silica at 800 °C, 12 kbar, from solubility measurements on SiO_2-buffering mineral assemblages. Contributions to Mineralogy and Petrology, 146, 135–143.
——— (2006) Solubilities of corundum, wollastonite and quartz in H_2O-NaCl solutions at 800 °C and 10 kbar: Interaction of simple minerals with brines at high pressure and temperature. Geochimica et Cosmochimica Acta, 70, 5571–5582.
Novgorodov, P.G. (1975) Solubility of quartz in H_2O-CO_2 mixtures at 700 °C and pressures of 3 and 5 kbar. Geochemistry International, 12, 122–126.
Shettel, D.L. (1974) The solubility of quartz in supercritical H_2O-CO_2 fluids. M.S. thesis, Pennsylvania State University, University Park.
Shmulovich, K.I., Graham, C.M., and Yardley, B.W.D. (2001) Quartz, albite and diopside solubilities in H_2O-NaCl and H_2O-CO_2 fluids at 0.5–0.9 GPa. Contributions to Mineralogy and Petrology, 141, 95–108.
Shmulovich, K.I., Yardley, B.W.D., and Graham, C.M. (2006) Solubility of quartz in crustal fluids: experiments and general equations for salt solutions and H_2O-CO_2 mixtures at 400–800°C and 0.1–0.9 GPa. Geofluids, 6, 154–167.
Walther, J.V. and Orville, P.M. (1983) The extraction-quench technique for determination of the thermodynamic properties of solute complexes; applications to quartz solubility in fluid mixtures. American Mineralogist, 68, 731–741.
Zotov, N. and Keppler, H. (2002) Silica speciation in aqueous fluids at high pressures and temperatures. Chemical Geology, 184, 71–82.